CHEMISTRY
A EUROPEAN JOURNAL

DOI: 10.1002/chem.200900795

VIP

Trisilyl-Substituted Vinyl Cations

Andrea Klaer,[a] Yvonne Syha,[b] Hamid Reza Nasiri,[c] and Thomas Müller*[a]

Dedicated to Professor Yitzhak Apeloig in occasion of his 65th birthday

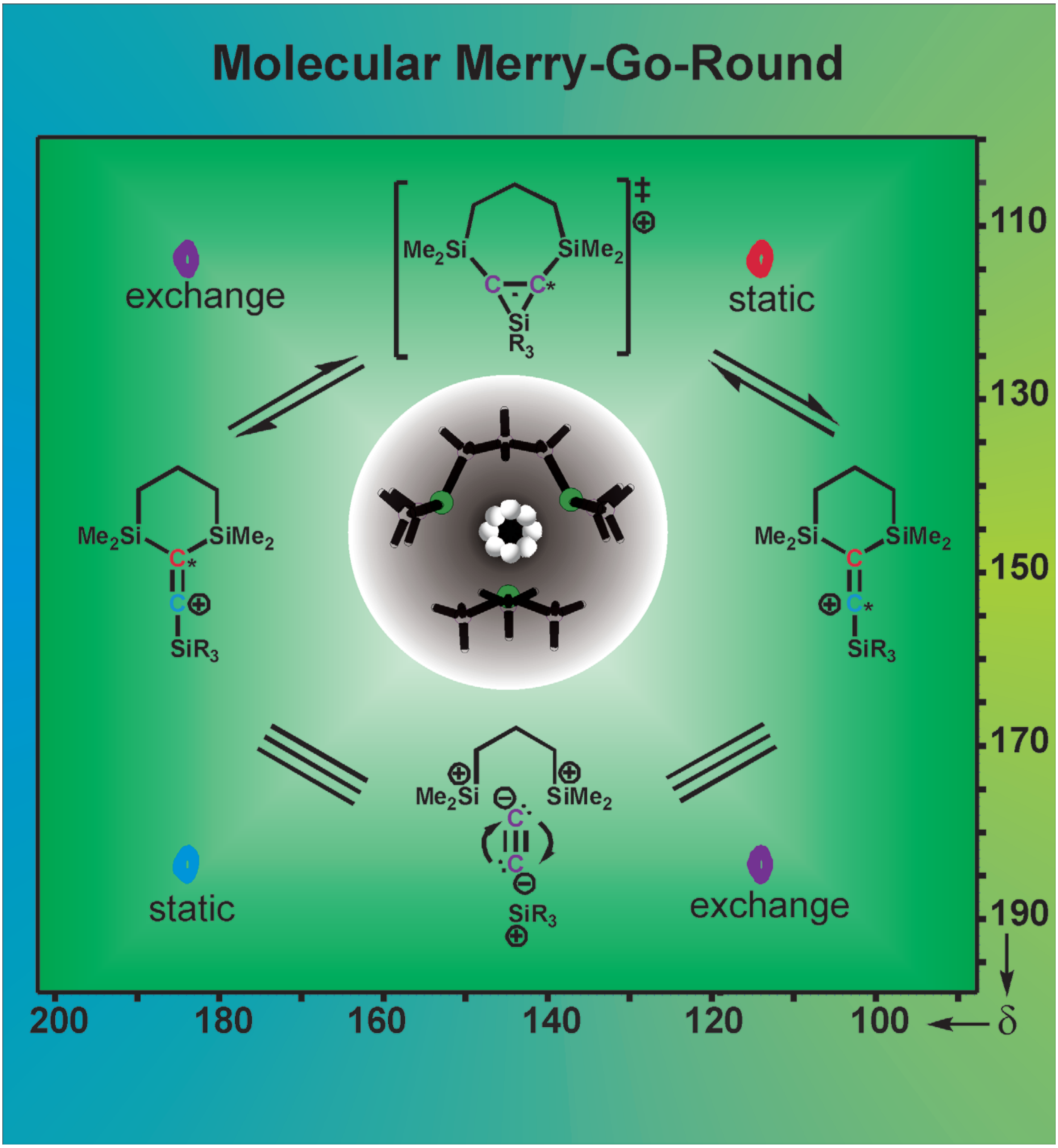

Abstract: A series of β,β-disilyl-substituted vinyl cations were prepared by intramolecular addition of transient silylium ions to C≡C triple bonds. The vinyl cations were isolated from hydrocarbon solutions as tetrakis(pentafluorophenyl) borates at room temperature. The substituents directly attached to the positively charged carbon atom were varied from *tert*-butyl- to trialkylsilyl- to trialkylgermyl groups. The cations were identified by their characteristic ^{13}C and ^{29}Si NMR data. The NMR investigations revealed for β,β-disilyl-α-germyl- and trisilyl-substituted vinyl cations a highly dynamic structure in which both vinylic carbon atoms undergo an intramolecular exchange process which is fast on the NMR time scale at room temperature. NMR studies using a doubly ^{13}C-labeled vinyl cation suggest as mechanism for this exchange process a rotation of the dicarbyne $C≡C^{2-}$ unit within the triangle defined by the three cationic silyl fragments. Therefore the dynamic structure indicated for trisilyl- or disilylgermyl-substituted vinyl cations parallels the situation found for the parent vinyl cation, the protonated acetylene.

Keywords: ab initio calculations · carbocations · density functional calculations · Group 14 elements · NMR spectroscopy

Introduction

Vinyl cations,[1] carbenium ions of the general formula $R_3C_2^+$, usually adopt a configuration in which the positively charged sp-hybridized carbon atom is linearly coordinated and the second, sp^2-hybridized carbon atom has trigonal planar coordination environment. For substituted vinyl cations (R ≠ H), this classical Y-shaped structure is predicted by quantum mechanical calculations to be that of the most stable isomer.[2] This prediction is confirmed by the stereochemical outcome of vinylic S_N1-type substitution reactions[3] and by the results of NMR investigations of persistent vinyl cations.[4–7] Final experimental proof for the classical vinyl cation structure came from recent X-ray diffraction investigations of salts of vinyl cations **1a** and **2** with weakly coordinating counter anions.[5]

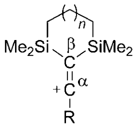

n = 0,1,2

1

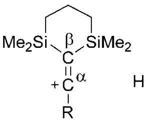

1a: R = *t*Bu
2: R = cyclopropyl

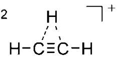

3

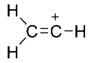

4

Most notably, the parent $C_2H_3^+$ ion adopts a different structure. All high level quantum mechanical investigations conclude that the most stable isomer of the $C_2H_3^+$ ion is the protonated acetylene **3** and that the Y-shaped vinyl cation isomer **4** represents either only a shallow minimum on the potential energy surface (PES) or is the transition state for a degenerate hydrogen-interchange process in **3**.[2b,9] The barrier for this degenerate "merry-go-round" process is uniformly predicted to be very small (less than 17 kJ mol^{-1}), which indicates a highly fluxional structure for the $C_2H_3^+$ ion. In agreement with these conventional theoretical methods, ab initio molecular dynamic simulations that treat the nuclei as classical and quantum particles find a quasi-planar quantum ground state of $C_2H_3^+$ with anisotropic delocalization of the protons due to zero-point quantum effects.[10] Finally, advanced infrared[11–12] and millimeter wave[13–16] spectroscopy clearly favor a bridged structure subject to proton tunneling and the deduced rotational constants as well as the barrier height agree with theoretical predictions for the hydrogen-bridged cation **3**.[17]

Silylium ions, R_3Si^+ behave similar to protons as substituents.[18] In both types of cations positive charge is accumulated in a relatively small region in space. This high positive charge accumulation results in a high reactivity of the cations towards all accessible nucleophiles, and in consequence these ions are hard to observe as free entities unfettered by any interaction in condensed media.[19] This similarity between protons and silylium ions prompted us to investigate the structure of trisilyl-substituted and related vinyl cations by computational and experimental methods. The straightforward access of cyclic β,β-disilyl-substituted vinyl cations of the general type **1** by intramolecular addition of transient silylium ions to a C≡C triple bond can in principle be extended to a large variety of vinyl cations which have different substituents R directly attached to the positively charged carbon atom C$^{\alpha}$. Previously, we reported the synthesis of vinyl cations **1** with cation stabilizing substituents such as alkyl, cyclopropyl or aryl in the α-position.[6–8,20] In this report, we extend the series of vinyl cations **1** to cations with substituents R such as silyl and germyl which in principle have a destabilizing effect compared to alkyl groups on the stability of a vinyl cation in the α-position. Therefore, we synthesized and characterized trisilyl, ($R = SiR_3$), disilyl germyl ($R = GeR_3$) and, for comparison, disilyl alkyl (R =

---

[a] Dipl.-Chem. A. Klaer, Prof. Dr. T. Müller
Institut für Reine und Angewandte Chemie
Carl von Ossietzky Universität Oldenburg
Carl von Ossietzky Strasse 9–11, 26211 Oldenburg (Germany)
E-mail: thomas.mueller@uni-oldenburg.de

[b] Dr. Y. Syha
Institut für Anorganische und Analytische Chemie
Johann Wolfgang Goethe-Universität Frankfurt/Main
Marie-Curie-Strasse 11, 60439 Frankfurt (Germany)

[c] Dr. H. R. Nasiri
Department of Chemistry, University of Cambridge
Lensfield Road, Cambridge, CB2 1EW (UK)

Supporting information for this article is available on the WWW under http://dx.doi.org/10.1002/chem.200900795.

*t*Bu) substituted vinyl cations **1** in order to probe their stability, their structure and the dynamic in these vinyl cations in dependence on the ring size and on the α-substituent R. The experimental studies are supported and extended by quantum mechanical calculations on structures and energies for vinyl cations **1** and for the parent $(H_3Si)_3C_2^+$ cation.

Results and Discussion

Synthesis: The precursor alkynyl silanes **5** were synthesized according to standard synthetic protocols,[6–8] which are described in detail in the Supporting Information. As described previously for cation **1a** and related cations, treatment of the precursor **5** with trityl cation in benzene or toluene gave the corresponding cyclic vinyl cations **1b–e**, **h**, **i**, **m–p** (see Scheme 1).[6–8] The counteranion was in all cases tetrakis(pentafluorophenylborate) (TPFPB). Interestingly, the polysilyl- and triphenylsilyl-substituted alkynes **5f** and **5g** did not give a vinyl cation upon treatment with trityl cation. In these cases several unidentified products were detected by NMR spectroscopy. The vinyl cation salts **1**·TPFPB were isolated as white or slightly brown amorphous or microcrystalline solids. All attempts to grow crystals from the **1**·TPFPB salts using different solvents such as fluorinated or chlorinated arenes failed. Similarly, all attempts to use anions such as halogenated carboranates to obtain crystals from **1**·$[CB_{11}H_6X_6]^-$ (X = Cl, Br)[8] which are suitable for X-ray diffraction were unsuccessful. The salts **1**·TPFPB form liquid clathrates of high salt concentrations with arene solvents which faciliate the NMR spectroscopic investigations. These clathrates remain liquid down to temperatures of about −30–−40 °C. At lower temperatures the clathrates become solid. No marked solvent effects on the NMR chemical shifts can be detected as long as aromatic hydrocarbons are used (see Table 1). Addition of solvents of higher donicity as, for example, methylene chloride even at temperatures as low as −50 °C leads to decomposition of the vinyl cations. Addition of acetonitrile to a benzene solution of **1b** TPFPB results in the clean formation of acetonitrilium ion **6** (see Table 1).

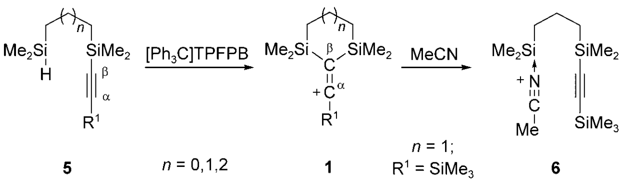

Scheme 1. Synthesis of vinyl cations **1** and nitrilium ion **6** (For the compound numbering see Table 1).

The thermal stability of the vinyl cation salts **1**·TPFPB strongly depends on the substituent R. The *tert*-butyl substituent confers to the vinyl cation a high stability.[8a] As a result solutions of cations **1a**,**m**,**o** in arene solvents show no sign of decomposition even after storage for days at room temperature. In agreement with previous theoretical predictions,[21] the silyl- and germyl-substituted vinyl cations **1b–e**,**h**,**i**,**n**,**p** are significantly less stable. In the case of the trimethylsilyl-substituted vinyl cations **1b**,**n**,**p** the decomposition rate increases with increasing ring size. That is, the five-membered ring cation **1n** is stable at 60 °C in toluene while the seven-membered ring cation **1p** slowly decomposes even at 0 °C into unidentified products. Substitution with more bulky substituted silyl groups does not increase the thermal stability of the cations significantly. For example, the *tert*-butyldimethylsilyl-, the triisopropylsilyl- and the tris(trimethylsilyl)-substituted vinyl cations **1c–e** are only marginally more stable than the trimethylsilyl-substituted cation **1b** and decompose at temperatures above 40 °C.

NMR spectroscopic characterization: The ^{13}C NMR spectroscopic parameter of the *tert*-butyl-substituted vinyl cations **1m** and **1o** (see Table 1 and Experimental Section) closely resemble those reported previously for vinyl cation **1a**.[8] Therefore, these cations clearly adopt a classical vinyl cation ground-state structure. The $C{=}C^+$ unit of the vinyl cation is readily identified by the low-field resonance of the positively charged C^α atom at $\delta\ ^{13}C = 198.5–204.6$ ppm and that attributed to the trigonal C^β atom at $\delta\ ^{13}C = 74.9–77.0$ ppm. The unusual small $^1J(C^\beta,Si)$ coupling constant ($^1J(C^\beta,Si)$ = 16.7 (**1o**), and 20.2 Hz (**1m**)) is typical for the C^β–Si bond in these cations and is a consequence of the reduced bond order due to delocalization of electron density from the σ-Si–C^β bond to the formally empty 2p orbital at the positively charged C^α atom.[7,8] In both *tert*-butyl-substituted vinyl cations, **1m** and **1o**, the silicon atoms are deshielded compared with **1a** ($\delta\ ^{29}Si = 28.9$ (**1a**), 70.8 (**1m**), 38.0 (**1o**)). In particular the significant low-field shift detected for the compound **1m** is remarkable, but can be attributed at least in part to the increased ring strain in the five-membered ring compound **1m** compared with 1,3-disilahexane compound **1a**. Similar deshielding effects on $\delta\ ^{29}Si$ NMR chemical shifts have been previously described for neutral 1,3-disilacyclopentanes compared with 1,3-disilacyclohexanes.[22]

The close accordance with the ^{13}C NMR data for the α-trialkylsilyl-substituted vinyl cations **1b–e**, collected at temperatures below 0 °C, to those of **1a** (see Table 1) clearly indicates classical Y-shaped ground state structures also for these trisilyl-substituted vinyl cations. For all four cations, **1b–e**, the $C{=}C^+$ unit is indicated by the low-field resonance for the C^α atom at $\delta\ ^{13}C(C^\alpha) = 231.3–181.7$ and by the relatively high-field shifted signal for C^β ($\delta\ ^{13}C(C^\beta) = 116.1–108.6$). The ^{29}Si NMR chemical shift detected for the β-$SiMe_2$ groups are in the expected region for β,β-disilyl-substituted vinyl cations ($\delta\ ^{29}Si(SiMe_2) = 19.9$-26.9, see Table 1)[6–8] while the ^{29}Si NMR signals for the α-trialkylsilyl groups in cations **1b–d** appear at higher field ($\delta\ ^{29}Si(Si) = -1.1–7.7$).[23] Interestingly, both types of silicon nuclei in cations **1b–e** are deshielded compared with the respective precursor bissilylalkynes **5b–e**. The deshielding of the β-silicon atoms upon ionization is large ($\Delta\delta\ ^{29}Si = 39.1–45.3$)[24] and can be rationalized by the occurrence of β-Si–C hyperconju-

Table 1. NMR chemical shifts δ and experimental activation energies E_A for C^α, C^β interchange in alkyl-, silyl- and germyl-substituted vinyl cations **1**.[a]

Cpd	n	R	δ $^{13}C^\alpha$	δ $^{13}C^\beta$	δ $^{29}SiMe_2$	δ $^{13}C(CH_2)$	δ $^{29}Si(R)$	E_A[b]
1a[c,d]	1	*t*Bu	202.7	75.5	28.9	16.2; 15.2		
1b[e]	1	$SiMe_3$	184.1	114.1	21.4	15.9; 15.8	−1.1	(56.0±3.3)
1b[c]	1	$SiMe_3$	–	–	21.1	16.1; 16.1	−1.2	
1b[c,i]	1	$SiMe_3$	--	–	21.4	15.8; 15.8	−1.1	
1c[f]	1	$SiMe_2$*t*Bu	181.7	116.1	19.9	16.1; 15.9	6.4	(53.1±5.4)
1d[f]	1	Si*i*Pr_3	209.9	109.8	26.9	16.0; 15.9	7.7	(53.5±5.4)
1e[i]	1	$Si(SiMe_3)_3$	231.3	108.6	22.3	16.0; 15.8	−95.7, −4.3	
1f	1	Si(Si*t*Bu$Me_2)_3$						
1g	1	$SiPh_3$						
1h[c]	1	$GeMe_3$	151.2	151.2	16.9	16.1; 16.1		(29.7±1.3)
1h[c,i]	1	$GeMe_3$	151.0	151.0	16.9	15.8; 15.8		
1i[c]	1	Ge*i*Pr_3	160.9	160.9	22.2	15.9; 15.9		(28.1±4.9)
1k	1	Sn*n*Bu_3						
1l	1	$Sn(cy\text{-}hex)_3$						
1m[c]	0	*t*Bu	198.5	74.9	70.8	12.7		
1n[f]	0	$SiMe_3$	161.1	127.6[j]	47.5	13.7	−0.3	
1o[g]	2	*t*Bu	204.6	77.0	38.0	24.4; 17.9		
1p[h]	2	$SiMe_3$	153.0	153.0	28.2	24.0; 16.1	0.3	
6[c,i]	1	$SiMe_3$	115.2	112.3	33.5; −17.9	19.3; 17.6; 16.9	−19.0	

[a] In $[D_8]$toluene. [b] Activation energies in $kJ\,mol^{-1}$. [c] At $T = 300$ K. [d] From ref. [8]. [e] At $T = 243$ K. [f] At $T = 273$ K. [g] At $T = 263$ K. [h] At $T = 258$ K. [i] In $[D_6]$benzene. [j] The ^{13}C NMR signal for C^β in $[D_8]$toluene was detected using a $^{13}C\{^1H\}$ INEPT pulse sequence using 12 CH protons of the two $SiMe_2$ groups and an estimated $^2J(C^\beta H) = 5$ Hz.

gation and therefore localization of positive charge at the β-silicon atoms.[6,7] The deshielding of the α-silicon atom is smaller, but still significant ($\Delta\delta$ $^{29}Si = 5.8$–24.6) and might be a result of the electron-withdrawing effect of the neighboring positively charged carbon atom.

The ^{13}C NMR signals of the carbon atoms C^α and C^β in **1b**–**e** show kinetic line broadening. That is, while at low temperatures ($T = 243$ K) relative narrow signals were detected, the lines broaden at higher temperatures and they finally disappear in the base line at temperatures around $T = 273$ K. This process is fully reversible and after cooling to $T = 253$ K both ^{13}C NMR signals for the $C{=}C^+$ unit are clearly visible. Up to temperatures $T = 373$–383 K no time averaged signal could be detected, at that temperatures, however, decomposition of the trisilyl-substituted vinyl cations becomes an important process. NMR investigations using $[^{13}C_2]$-**1b**·TPFPB, in which both vinylic carbon atoms were ^{13}C-labeled, allowed a deeper understanding of the dynamic processes in this cations. Two-dimensional exchange spectroscopy (2D EXSY)[25] at $T = 253$ K clearly indicated a side exchange between both vinylic carbon atoms in vinyl cation $[^{13}C_2]$-**1b** (see Figure 1). $^{13}C\{^1H\}$ NMR spectroscopic measurements at $T = 243$ K gave doublets at δ $^{13}C(C^\alpha) = 184.1$ and δ $^{13}C(C^\alpha) = 116.1$ ppm for both vinylic carbon atoms with a $^1J(C,C)$ coupling constant of $^1J(C,C) = 65$ Hz. This is significantly smaller than the coupling constant determined for the precursor alkyne $[^{13}C_2]$-**5b** ($^1J(C,C) = 103$ Hz). At higher temperatures the multiplet structure of the ^{13}C NMR signals merge into two broad signals (see Figure 1 for spectra at $T = 253$ K). Particular instructive are the $Si\{^1H\}$ NMR spectra taken from $[^{13}C_2]$-**1b**·TPFPB at various temperatures (see Figure 2). At low temperatures, both ^{29}Si NMR signals appear as doublets due to the coupling with one ^{13}C nuclei ($^1J(Si,C^\beta)(SiMe_2) = 12$ Hz and $^1J(Si,C^\alpha)(SiMe_3) = 41$ Hz). This observed coupling pattern is in agreement with a Y-shaped ground-state structure for $[^{13}C_2]$-**1b**. Above room temperature the multiplicity of both signals has changed to two triplets indicating the coupling with two equivalent ^{13}C atoms with about halved $^1J(Si,C)$ coupling constants ($^1J(Si,C^\beta)(SiMe_2) = 6$ Hz and $^1J(Si,C^\alpha)(SiMe_3) = 20$ Hz). Both ^{29}Si NMR chemical shifts are slightly temperature dependant ($\Delta T = 80$ K: $\Delta\delta$ $^{29}Si(SiMe_3) = 0.9$; $\Delta\delta$ ^{29}Si $(SiMe_2) = 2.3$, see Figure 2).

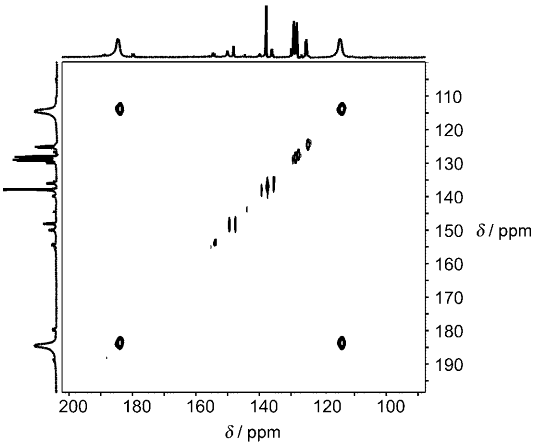

Figure 1. $^{13}C\{^1H\}$ 2D EXSY phase sensitive contour map obtained at 125.705 MHz with a mixing time of 500 ms at $T = 253$ K of $[^{13}C_2]$-**1b** TPFPB in $[D_8]$toluene.

We attribute this dynamic behavior of the vinyl cations **1b**–**e** to a degenerate rotation of the central $C^\beta{\equiv}C^\alpha$ dicarbyne unit within the triangle of the three silicon substituents, in which both carbon atoms are interchanged via the silyl-bridged transition states **7b**–**e** (see Scheme 2). The activation energies E_A for this processes were extracted from line-shape analysis in the slow-exchange regime and were determined to be $E_A = 53.1$–$56.0\ kJ\,mol^{-1}$ (see Table 1 and the Supporting Information for details).

The intriguing difference between the static vinyl cation **1a** and the floppy molecule **1b** can be qualitatively understood when the relative energy of the respective transition state structure **7** is taken into account. Alkyl-bridging in **7a** is energetically clearly less favored than bridging by the silyl

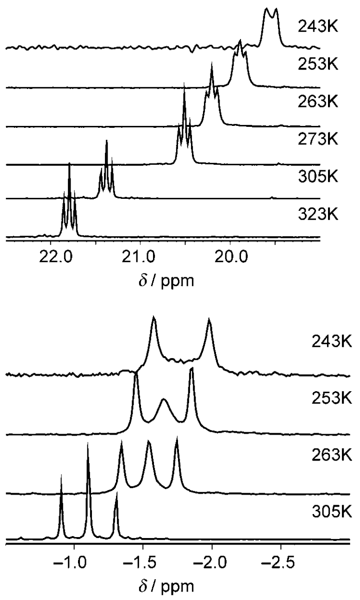

Figure 2. 99.305 MHz $^{29}Si\{^1H\}$ INEPT spectra of $[^{13}C_2]$-**1b**·TPFPB in $[D_8]$toluene. Top: Signals due to the $SiMe_2$ groups. Bottom: Resonances due to the $SiMe_3$ group.

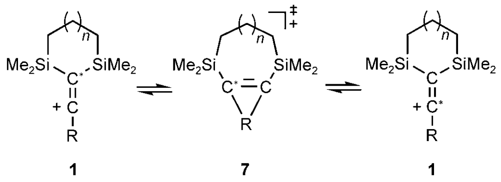

Scheme 2. Degenerate rotation of the C=C$^+$ unit in disilyl-substituted vinyl cations **1** via R-bridged transition states **7**.

group in **7b**, therefore the barrier for the rotation of the central C=C$^+$ unit is high for **1a**, while it is thermally accessible in the case of **1b** (and likewise for **1c–e**). Extending this rationalization, germyl substitution as in **1h** and **1i** should further decrease this barrier. The NMR spectroscopic parameter detected for the trialkylgermyl-substituted vinyl cation **1h** and **1i** at $T=303$ K are very similar to those found for the related cations **1a** and **1b** (see Table 1 and the Supporting Information), with the notable exception that for each cation for the carbon atoms C^α and C^β only one signal at room temperature was detected (**1h**: δ $^{13}C=151.2$; **1i**: δ $^{13}C=160.9$). This indicates that the degenerate rearrangement which interconverts the carbon atoms C^α and C^β in **1h**, **i**, is fast on the NMR time scale at ambient temperature. In both cases the ^{13}C NMR signal broadens considerably upon cooling, however, no coalescence and no line splitting could be observed before the sample becomes solid at $T=233$ K. The activation energy E_A for this rotation of the C=C$^+$ unit in the germyl-substituted vinyl cations **1h**, **i** had to be extracted solely from the data obtained in the fast exchange regime and was found to be $E_A=29.7$ kJ mol^{-1} (**1h**) and $E_A=28.1$ kJ mol^{-1} (**1i**).[26] The results of the NMR investigations for vinyl cations **1a–e**, **h**, **i** suggest that the energy difference between the classical Y-shaped vinyl cation isomer **1** and the bridged species **7** decreases going from alkyl substituents to silyl and finally to germyl groups. All attempts to prepare stannyl-substituted vinyl cations failed, probably due to the fast destannylation of the stannylalkyne precursors **5k**,**l** during the preparation of the cation.

A second factor which severely influences the barrier for the rotation of the central C=C$^+$ unit in cations of type **1** is the ring size. Transition-state structures **7** with larger rings are better suited to accommodate the carbon atoms C^α and C^β with a formal hybridization state between sp and sp^2. Therefore, the barrier for the rotation of the central C=C$^+$ unit in vinyl cations **1** is expected to increase with decreasing lengths n of the alkyl chain. Therefore, we synthesized the TPFPB salt of trisilyl-substituted vinyl cation **1n** which has a five-membered disilaheterocycle ($n=0$), and of the trisilyl-substituted vinyl cation **1p** with a seven-membered disilaheterocycle ($n=2$) (see Scheme 2). The ^{13}C and ^{29}Si NMR chemical shifts found for the five-membered ring cation **1n** clearly indicate the classical Y-shaped vinyl cation structure (see Table 1 and Supporting Information) and the detected ^1J(C,Si) coupling constants ($^1J(C^\beta,Si)=17.6$ Hz and $^1J(C^\alpha,Si)=38.6$ Hz) are in agreement with those determined for the $[^{13}C_2]$-**1b** and provide further evidence for its structure. In contrast to the six-membered ring cation **1b**, however, the ^{13}C NMR spectra of five-membered ring cation **1n** show at room temperature no kinetic line broadening. Even at 70 °C, when the cation **1n** starts to decompose no kinetic line broadening of the ^{13}C NMR signals of the carbon atoms C^α and C^β could be observed. The NMR data obtained for the trimethylsilyl-substituted seven-membered ring cation **1p** ($n=2$) are similar to that of the trialkylgermyl-substituted vinyl cations **1h**, **i** and to those of the silyl-substituted vinyl cations **1b–e** and are therefore in agreement with a classical Y-shaped vinyl cation ground state structure. In particular, the ^{13}C NMR spectrum of the cation **1p** shows even at $T=243$ K only one time-averaged signal for the two vinylic carbon atoms. At lower temperatures the $[D_8]$toluene solution starts to solidify. The apparent limitations, the thermolability of cation **1n** and the relative high freezing point of the clathrate of the salt **1p**·TPFPB with $[D_8]$toluene, clearly prevent an accurate determination of the activation barriers for the carbon atom interchange process in the trisilyl cations **1n** and **p**. Nevertheless, these experiments can be used to confirm qualitatively the expected relation between ring size of the cation and activation barrier.

Computational part:[27] In order to reach a principal understanding of the nature of experimentally investigated tris(trialkylsilyl)-substituted vinyl cations **1b–e**, **n**, **p** the structures of several isomers of the parent trisilyl vinyl cation $(H_3Si)_3C_2^+$ (**8**) were computed at the density functional B3LYP/6-311G(2d,p)[28] and at the ab initio MP2/6-311G-(2d,p) and CCSD/cc-pvtz levels of theory.[29–32] In particular, the bridged isomer **8a** of C_s symmetry and the classical Y-shaped vinyl cation structure **8b** were investigated (see Figure 3). Both standard methods, B3LYP and MP2, predict for each of the two isomers, **8a** and **8b**, very similar geometries. The methods differ however partly in the description of the nature of the stationary points (see Table 2). While the Y-shaped isomer **8b** is found to be the transition state for in-plane silyl migration by both methods, the silylbridged isomer **8a** is the ground state of the trisilyl vinyl cation **8** with the ab initio MP2 method, but it is a transition state at the hybrid density functional B3LYP level of theory. At the B3LYP level of theory the ground state of the trisilyl vinyl cation **8** adopts a quite unsymmetrical structure **8c** (Figure 3). Qualitatively, the geometry of isomer **8c** is best described as a hybrid between the classical Y-shaped vinyl cation geometry and the silyl-bridged structure. The most significant structural feature of **8c** is the occurrence of two different β-silyl groups with clearly different Si–C bond distances (205.4 and 191.7 pm) and markedly distinct bond angles α(C$^{\alpha}$C$^{\beta}$Si) (90.9 and 152.4°).

Table 2. Relative energies (kJ mol^{-1}) of several isomers of trisilyl vinyl cation **8** at different levels of theory (number of imaginary frequencies in square brackets and size of the imaginary frequency in parenthesis).

	8a[a]	**8b**	**8c**
B3LYP/6-311G(2d,p)	0; [1], (−124)	−0.9; [1], (−41)	−2.9; [0]
MP2/6-311G(2d,p)	0; [0]	21.4; [1] (−82)	
CCSD/cc-pvdz	0	7.2	
CCSD(T)/cc-pvtz//B3LYP[b]	0	12.1	0.8
CCSD(T)/cc-pvtz//MP2[b]	0	13.3	

[a] Absolute energies of **8a**: −949.88425 H, B3LYP/6-311G(2d,p); −948.11521 H, MP2/6-311G(2d,p); −948,30916 H, CCSD(T)/cc-pvtz//B3LYP/6-311G (2d,p); −948.30939, CCSD(T)/cc-pvtz//MP2/6-311G-(2d,p). [b] A 6-311G(2d,p) basis set was used.

The isomers **8a** and **8b** are the only stationary points at the MP2 level along a reaction coordinate which allows for the interchange of the silyl groups in cation **8**. The barrier for this process which converts two equivalent cations **8a** via the transition state **8b** is 21.4 kJ mol^{-1} and a potential energy scan along the reaction coordinate for the in-plane migration of the silyl groups around the central carbyne core confirms the single minimum potential at the MP2 level (see Figure 4).

In agreement with the larger number of stationary points located, a similar potential energy scan at the B3LYP/6-311G(2d,p) level of theory suggests a more complicated reaction coordinate for the degenerate silyl migration in trisilyl vinyl cation **8**. Equivalent unsymmetrical ground-state structures **8c** are connected via the silyl-bridged transition state **8a** or via the nearly symmetric Y-shaped classical vinyl cation structure **8b**. These calculations reveal the "floppy" nature of trisilyl vinyl cation **8**. The located stationary points on the PES are all very near in energy, the highest barrier at B3LYP/6-311G(2d,p) is less than 5 kJ mol^{-1} and at MP2/6-311G(2d,p) less than 22 kJ mol^{-1}. This allows large geometric displacements on only small energy costs. Coupled cluster single point calculations using a relatively large basis set of triple zeta quality (CCSD(T)/cc-pvtz) were used to obtain more reliable information about the nature of the different isomers of **8** and their relative energy differences. Single-point calculations were performed for all stationary points at the B3LYP and at the MP2 potential energy surface. The coupled cluster calculations predict that the silyl-bridged

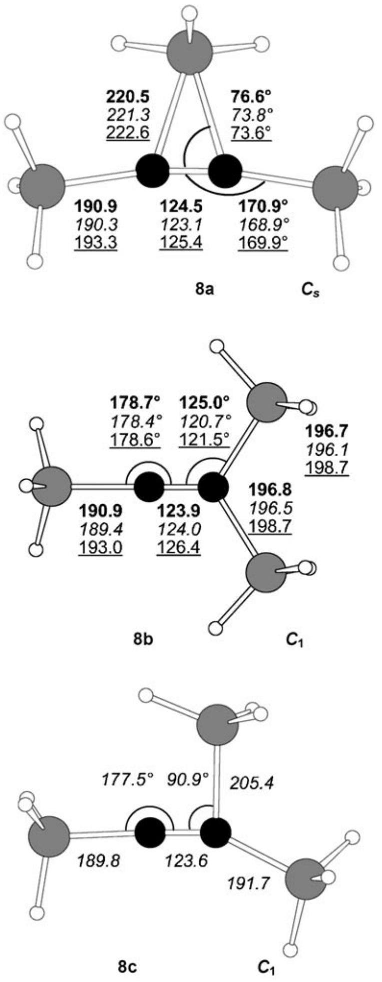

Figure 3. Calculated structures of the [(H$_3$Si)$_3$C$_2$]$^+$ cation **8**, obtained at the MP2/6-311G(2d,p) (bold), at the B3LYP/6-311G(2d,p) (italic) and at the CCSD/cc-pvdz (underlined) level of theory (Computed bond lengths in pm).

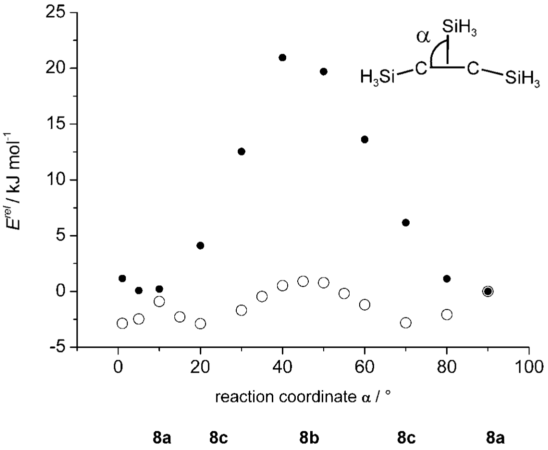

Figure 4. Calculated reaction path for the SiH$_3$ interchange in the [(H$_3$Si)$_3$C$_2$]$^+$ cation **8**, obtained at the MP2/6-311G(2d,p) (●) and at the B3LYP/6-311G(2d,p) (○) level of theory.

isomer **8a** is more stable than the classical Y-shaped vinyl cation **8b** by 13.3 kJ mol^{-1} (CCSD(T)/cc-pvtz//MP2/6-311G-(2d,p), 12.1 kJ mol^{-1} at CCSD(T)/cc-pvtz//B3LYP/6-311G-(2d,p)) and also the unsymmetrical isomer **8c** is predicted to be less stable than **8a** by 0.8 kJ mol^{-1} (at CCSD(T)/cc-pvtz//B3LYP/6-311G(2d,p)). Therefore our most reliable calculations predict for the trisilyl vinyl cation **8** a silyl bridged ground state **8a** with relatively small barriers for silyl migration around the central carbyne core via the classical vinyl cation isomer **8b**. This situation is reminiscent to that found for the parent $C_2H_3^+$ cation with a hydrogen bridged ground state and very small barriers for hydrogen interchange.[9–16]

The presence of alkylidene bridges $(CH_2)_{n+2}$ ($n=0$–2) between two silicon atoms in the experimentally investigated cations **1** is expected to stabilizes the Y-shaped vinyl cation structure compared to its silyl-bridged isomer. Consequently, density functional calculations at the B3LYP/6-311G(2d,p) level of theory predict a classical Y-shaped ground-state structure for the tris(trialkylsilyl)-substituted vinyl cation **1b** (see Figure 5a and Table 3), in qualitative agreement with the results of the low temperature NMR studies for [$^{13}C_2$]-**1b**·TPFPB. In contrast calculations at the MP2/6-311G(2d,p) level of theory predict an essentially symmetrically bridged structure for cation **1b** with the silicon atom Si$^{\beta1}$ strongly bent towards the C≡C triple bond (see Figure 5b). These significant differences between the structures obtained by both methods are even more remarkable in view of the close agreement between both methods which is usually obtained, for example for the geometry of the closely related *tert*-butyl, or cyclopropyl-substituted vinyl cations **1a** and **2**.[8] Similar as found for the trisilyl vinyl cation **8** the mode for bending the bond angle $\alpha(C^{\alpha}C^{\beta}Si^{\beta1})$ in vinyl cation **1b** is rather weak. That is, the energy difference between both theoretically predicted structures for vinyl cation **1b** is merely 16 kJ mol^{-1} (at MP2(fu)/6-311G(2d,p); 11 kJ mol^{-1} at B3LYP/6-311G(2d,p)).[33] In addition, the activation energy for the degenerate Si$^{\beta1}$/Si$^{\beta2}$ exchange process via the C_s symmetric transition state **9b** (see Figure 5c) is rather small (16.0 kJ mol^{-1} at MP2/6-311G(2d,p), 1.4 kJ mol^{-1} at B3LYP/6-311G(2d,p)). This small barrier and the overall flat potential energy surface suggest a time-averaged Y-shaped structure for cation **1b** in solution, regardless of the actual ground-state structure. This is in qualitative agreement with the NMR spectroscopic results that show only one signal for the two β-silicon atoms and with the observation of a duplet signal for the β-silicon atoms in the ^{29}Si NMR of [$^{13}C_2$]-**1b** at low temperatures. Further consequences that arise from the flatness of the potential energy surface for trisilyl-substituted vinyl cations **1b-e**, **n**, **p** are i) the determination of the molecular structures by theoretical methods is very demanding. As shown in Figure 5s,b standard quantum mechanical methods such as B3LYP and MP2 using a relative large basis set do not result in a conclusive result and higher correlation methods combined with larger basis sets seems to be appropriate;[34] ii) Steric interactions between substituents at Si$^{\alpha}$ and Si$^{\beta1}$ will severely influence the actual structure. Therefore, the use of less substituted model cations for the evaluation of the influence of higher theoretical methods on the structure prediction for cations **1** is of only little informative value.

Table 3. Calculated structural parameter of vinyl cations **1** at the B3LYP and MP2 level of theory (bond lengths r in pm, bond angles α in [°]) calculated activation barriers $\Delta E_A/\Delta G^{298}$ for the C$^{\alpha}$/C$^{\beta}$ interchange in these vinyl cations (in kJ mol^{-1}).

Compound		B3LYP/A[a]	MP2A[a]
1a	$r(C^{\alpha}{=}C^{\beta})$	123.8	
	$r(Si^{\beta1}{-}C^{\beta})$	200.1	
	$r(Si^{\beta2}{-}C^{\beta})$	197.3	
	$r(C^{\alpha}{-}Si^{\alpha})$	–	
	$\alpha(C^{\alpha}C^{\beta}Si^{\beta1})$	117.4	
	ΔE_A	167.2	
	ΔG^{298}	159.3	
1b	$r(C^{\alpha}{=}C^{\beta})$	123.8	124.9
	$r(Si^{\beta1}{-}C^{\beta})$	202.3	218.2
	$r(Si^{\beta2}{-}C^{\beta})$	196.2	191.0
	$r(C^{\alpha}{-}Si^{\alpha})$	190.7	191.1
	$\alpha(C^{\alpha}C^{\beta}Si^{\beta1})$	111.7	78.6
	ΔE_A	55.5	46.6
	ΔG^{298}	57.0	
1h	$r(C^{\alpha}{=}C^{\beta})$	123.8	
	$r(Si^{\beta1}{-}C^{\beta})$	202.3	
	$r(Si^{\beta2}{-}C^{\beta})$	196.2	
	$r(C^{\alpha}{-}Si^{\alpha})$	–	
	$\alpha(C^{\alpha}C^{\beta}Si^{\beta1})$	110.8	
	ΔE_A	34.3	
	ΔG^{298}	35.3	
1n	$r(C^{\alpha}{=}C^{\beta})$	123.7	124.8
	$r(Si^{\beta1}{-}C^{\beta})$	200.4	221.7
	$r(Si^{\beta2}{-}C^{\beta})$	198.3	191.3
	$\alpha(C^{\alpha}C^{\beta}Si^{\beta1})$	123.6	76.6
	$r(C^{\alpha}{-}Si^{\alpha})$	190.4	191.3
	ΔE_A	75.9	72.7
	ΔG^{298}	77.8	
1p	$r(C^{\alpha}{=}C^{\beta})$	124.0	124.9
	$r(Si^{\beta1}{-}C^{\beta})$	202.8	226.7
	$r(Si^{\beta2}{-}C^{\beta})$	196.8	190.8
	$\alpha(C^{\alpha}C^{\beta}Si^{\beta1})$	109.5	70.6
	$r(C^{\alpha}{-}Si^{\alpha})$	190.8	191.7
	ΔE_A	26.7	17.9
	ΔG^{298}	23.6	

[a] Basis set A: 6-311G(2d,p).

A situation quite similar to that for cation **1b** is found for the tris(trialkylsilyl)-substituted vinyl cations **1n** and **1p**. In both cases MP2 and B3LYP computations result in qualitative different structures with a significant more pronounced interaction of one β-silicon atom and the positively charged carbon atom C$^{\alpha}$ predicted by the MP2 method. This is shown most prominently with the bond angle $\alpha(C^{\alpha}C^{\beta}Si^{\beta1})$. The theoretical prediction of this parameter differs by 33.1° (for **1b**) to 47.0° (for **1n**) (see Table 3 and the Supporting Information for more details).

By contrast, both standard methods, B3LYP and MP2 predict for the transition state **7b** of the experimentally observed C$^{\alpha}$/C$^{\beta}$ interchange in vinyl cation **1b** very similar structures (see Figure 5d). The most remarkable feature of this transition state is that the α-trimethylsilyl group bridges nearly symmetrically the C≡C triple bond. Therefore this transition state structure for the C$^{\alpha}$/C$^{\beta}$ exchange in **1b** closely resembles the ground-state structure of protonated acety-

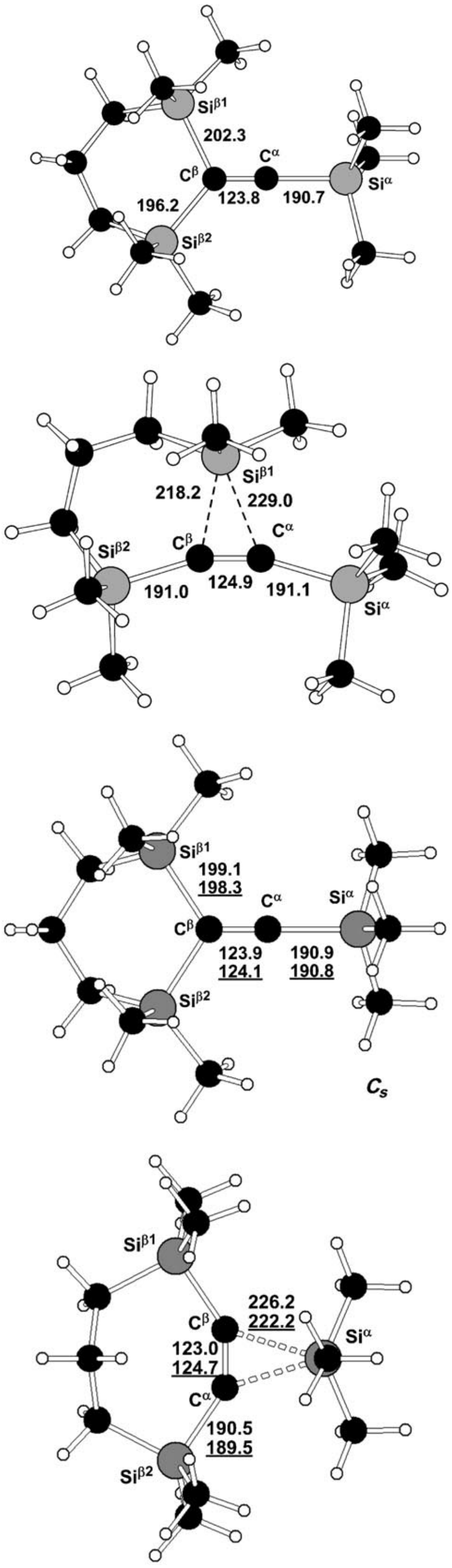

Figure 5. a) Computed molecular structure of vinyl cation **1b** (at B3LYP/6-311G(2d,p)); b) Computed molecular structure of vinyl cation **1b** (at MP2/6-311G(2d,p). c) Computed structure of the transition state **9b** for the equilibration of $Si^{\beta1}/Si^{\beta2}$. d) Computed structure of the transition state **7b** for the $C^{\alpha}\equiv C^{\beta}$ interchange in **1b** (at B3LYP/6-311G(2d,p) and underlined at MP2/6-311G(2d,p).

lene **3**. The computed barrier E_A for the C^{α}/C^{β} exchange in **1b** is $E_A = 55.5\,kJ\,mol^{-1}$ (at B3LYP/6-311G(2d,p), $E_A = 46.6\,kJ\,mol^{-1}$ at MP2/6-311G(2d,p)). This is very close to those experimentally determined for tris(trialkylsilyl)-substituted vinyl cations **1b–d** ($E_A = 53.1–56.0\,kJ\,mol^{-1}$, see Table 1). Expectedly, for the trimethylgermyl-substituted vinyl cation **1h** a significantly smaller activation energy of $E_A = 35.3\,kJ\,mol^{-1}$ is predicted by the calculations, in agreement with the experimentally determined smaller barrier for C^{α}/C^{β} exchange process in **1h** ($E_A = 29.7\,kJ\,mol^{-1}$). In contrast, the activation energy E_A calculated for C^{α}/C^{β} interchange in the α-*tert*-butyl-substituted cation **1a** is high ($E_A = 167.2\,kJ\,mol^{-1}$) in agreement with the static structure of this cation found in the experiment. The calculations of the activation energies for C^{α}/C^{β} exchange in the series of the α-trimethylsilyl-substituted vinyl cations **1b**, **1n**, **1p** nicely confirms the trend found experimentally at room temperature (see Table 3). The increasing size of the disilaheterocycle comparing vinyl cations **1n**, **1b** and **1p** results in decreasing calculated activation energies E_A. This in accord with the static Y-shaped structure of **1n** deduced from the NMR experiments, and a C^{α}/C^{β} exchange process in cation **1b**, which is slow on the NMR time scale and with the same process being fast on the NMR time scale in **1p**.

Conclusions

A series of ten vinyl cations including trisilyl-substituted and β,β-disilyl-α-germyl-substituted cations have been prepared from the appropriate precursor disilane **5** by the intramolecular addition of a transient silylium ion to the C≡C triple bond. TPFPB salts of these cations are stable at room temperature in the solid state and in solution of aromatic hydrocarbons. Their identity was verified by NMR spectroscopy, which reveals for all investigated vinyl cations a classical Y-shaped ground state structure. In addition, the NMR spectroscopic results indicate for trisilyl and β,β-disilyl-α-germyl-substituted vinyl cations **1b–e**, **h**, **i**, **p** a highly dynamic structure. Both carbon atoms of the central CC unit in vinyl cations undergo at room temperature a degenerate exchange process which is fast on the NMR time scale. This exchange process can be best described as a rotation of the central dicarbyne unit $C{\equiv}C^{2-}$ within the triangle defined by the three positively charged silyl groups or, in the case of germyl-substituted vinyl cations **1h**, **i**, defined by silyl cations and one germyl cation (see Scheme 3).

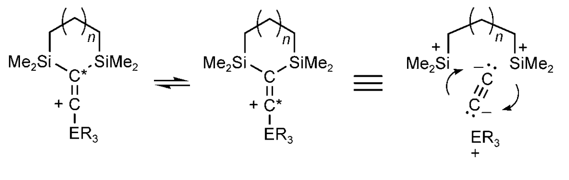

Scheme 3. Degenerate exchange process of the vinyl carbon atoms in vinyl cations **1** ($n = 1,2$; E = Si, Ge; R = alkyl, trialkylsilyl).

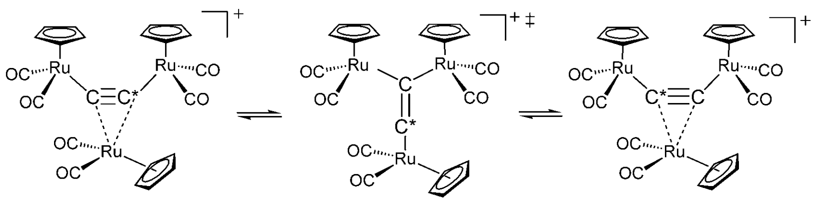

Scheme 4. Degenerate exchange process of the vinylic carbon atoms in the trinuclear ruthenium dicarbyne complex **10**.[35]

The barrier for this process strongly depends on the ring size and on the substituent in α-position in cations **1**. Small ring sizes and alkyl substituents increase the activation energy and larger rings and germyl substituents facilitate the exchange process.

The fluxional behavior of vinyl cations **1b**–**e**, **h**, **i**, **p** clearly parallels the results found recently for the cationic three-nuclear ruthenium complex **10**[35] and for protonated acetylene **3** (see Scheme 4) with the notable difference that the ground state configuration in both cations, **10** and **3**[10,36] is that of the bridged species and the classical Y-shaped vinyl cation configuration is only the transition state for the rotation process of the $C\equiv C^{2-}$ unit in the triangle of the three cationic fragments. Therefore, protonated acetylene **3**, trisilyl-substituted vinyl cations **1b**–**e**, **p** and the trinuclear ruthenium dicarbyne complex **10** provide an instructive example of an isolobal relationship in which the proton (no electron) can be replaced by the six electron main group fragment R_3Si^+ and by the sixteen electron transition metal fragment $[Ru(CO)_2(C_5H_5)]^+$ and molecular systems are obtained with similar structures and dynamics.

Acknowledgements

Prof. Dr. Uwe Rosenthal (Leibniz-Institut für Katalyse, Universität Rostock) is thanked for many helpful discussions. This work was supported by the Carl von Ossietzky Universität Oldenburg. The Wacker AG is thanked for generous gift of silanes. The computer centre of the Johann Wolfgang Goethe Universität Frankfurt/Main and Center for Scientific Computing (CSC) at the Universität Oldenburg is thanked for computer time.

---

[1] For a monograph on vinyl cations: *Dicoordinated Carbocations* (Eds.: Z. Rappoport, P. J. Stang), Wiley, New York, **1997**.

[2] a) R. Sustmann, J. E. Williams, M. J. S. Dewar, L. C. Allen, P. von R. Schleyer, *J. Am. Chem. Soc.* **1969**, *91*, 5350; b) for a review: Y. Apeloig, T. Müller in *Dicoordinated Carbocations* (Eds.: Z. Rappoport, P. J. Stang), Wiley, New York, **1997**, Chapter 2, p. 9.

[3] Review: T. Kitamura, H. Taniguchi, Y. Tsuno in *Dicoordinated carbocations* (Eds.: Z. Rappoport, P. J. Stang), Wiley, New York, **1997**, p. 321.

[4] a) F.-P. Kaufmann, H.-U. Siehl, *J. Am. Chem. Soc.* **1992**, *114*, 4937; b) H.-U. Siehl, F.-P. Kaufmann, K. Hori, *J. Am. Chem. Soc.* **1992**, *114*, 9343.

[5] a) H.-U. Siehl, F.-P. Kaufmann, Y. Apeloig, V. Braude, D. Danovich, A. Berndt, N. Stamatis, *Angew. Chem.* **1991**, *103*, 1546; *Angew. Chem. Int. Ed. Engl.* **1991**, *30*, 1479; b) H.-U. Siehl, T. Müller, J. Gauss, P. Buzek, P. von R. Schleyer, *J. Am. Chem. Soc.* **1994**, *116*, 6384.

[6] T. Müller, R. Meyer, D. Lennartz, H.-U. Siehl, *Angew. Chem.* **2000**, *112*, 3203; *Angew. Chem. Int. Ed.* **2000**, *39*, 3074.

[7] T. Müller, D. Margraf, Y. Syha, *J. Am. Chem. Soc.* **2005**, *127*, 10852.

[8] a) T. Müller, M. Juhasz, C. A. Reed, *Angew. Chem.* **2004**, *116*, 1569; *Angew. Chem. Int. Ed.* **2004**, *43*, 1543; b) A. Klaer, W. Saak, D. Haase, T. Müller, *J. Am. Chem. Soc.* **2008**, *130*, 14956.

[9] a) R. Lindh, J. E. Rice, T. J. Lee, *J. Chem. Phys.* **1991**, *94*, 8008; b) W. Klopper, W. Kutzelnigg, *J. Phys. Chem.* **1990**, *94*, 5625; c) C. Liang, T. P. Hamilton, H. F. Schaeffer III, *J. Chem. Phys.* **1990**, *92*, 3653.

[10] D. Marx, M. Parinello, *Science* **1996**, *271*, 179; for a previous Carr–Parinello study based on a exclusive classical treatment of the nuclei, see: J. S. Tse, D. D. Klug, K. Laasonen, *Phys. Rev. Lett.* **1995**, *74*, 876.

[11] M. W. Crofton, M.-F. Jagod, B. D. Rehfuss, B. D. , T. Oka, *J. Chem. Phys.* **1989**, *91*, 5193.

[12] T. Oka, *Philos. Trans. R. Soc. London Ser. A* **1988**, *324*, 81.

[13] M. Bogey, M. Cordonnier, C. Demunynck, J. L. Destombes, *Astrophys. J.* **1992**, *399*, L103.

[14] M. Bogey, M. Cordonnier, C. Demunynck, J. L. Destombes in *Structures and Conformations of Non-Rigid Molecules* (Eds.: J. Laane, M. Dakkouri, B. van der Veken, H. Oberhammer), Kluwer, Dordrecht, **1993**, p. 303.

[15] M. Bogey, M. Cordonnier, C. Demunynck, J. L. Destombes, *Can. J. Phys.* **1994**, *72*, 967.

[16] Review: C. Demuynck, *J. Mol. Spectrosc.* **1994**, *168*, 215.

[17] The results of coulomb explosion experiments which suggest a different structure are described in Z. Vager, D. Zajfman, T. Graber, E. P. Kanter, *Phys. Rev. Lett.* **1993**, *71*, 4319.

[18] a) D. Lauvergnat, P. C. Hiberty, D. Danovich, S. Shaik, *J. Phys. Chem.* **1996**, *100*, 5715; b) G. Sini, P. Maitre, P. C. Hiberty, S. S. Shaik, *J. Mol. Struct.* **1991**, *229*, 163.

[19] a) T. Müller, *Adv. Organomet. Chem.* **2005**, *53*, 155; b) M. Igarashi, M. Ichinohe, A. Sekiguchi, *J. Am. Chem. Soc.* **2007**, *129*, 12660; c) S. Yao, Y. Xiong, C. V. Wüllen, M. Driess, *Organometallics* **2009**, *28*, 1610; d) S. Duttwyler, Q.-Q. Do, A. Linden, K. K. Baldridge, J. S. Siegel, *Angew. Chem.* **2008**, *120*, 1743; e) T. Küppers, E. Bernhardt, R. Eujen, H. Willner, C. W. Lehmann, *Angew. Chem.* **2007**, *119*, 6462.

[20] T. Müller, D. Margraf, Y. Syha, H. R. Nasiri, C. Kaiser, R. Maier, B. Boltres, M. Juhasz, C. A. Reed in *Recent Developments in Carbocation and Onium Ion Chemistry* (Ed.: K. Laali), Oxford University Press, New York, **2007**, Chapter 3, p. 51.

[21] a) Y. Apeloig, A. Stanger, *J. Org. Chem.* **1982**, *47*, 1462; b) Y. Apeloig, A. Stanger, *J. Org. Chem.* **1983**, *48*, 5413.

[22] D. Seyferth, H. Friedrich, *Z. Naturforsch. B* **1994**, *49*, 1818.

[23] The data for cation **1e** are due to the different sustitution pattern not applicable.

[24] $\Delta\delta$ ^{29}Si was calculated according to: $\Delta\delta\ ^{29}\mathrm{Si} = \delta\ ^{29}\mathrm{Si}(\mathbf{1}) - \delta\ ^{29}\mathrm{Si}(\mathbf{5})$.

[25] S. Berger, S. Braun, *200 and More NMR Experiments*, Wiley-VCH, Weinheim, **1998**, p. 445.

[26] To calculate the exchange rate for **1h** the frequency difference $\Delta\nu$ between C^{α} and C^{β} obtained for **1b** was used, and for **1i** the frequency difference measured for **1d** was used. The errors given in Table 2 are calculated from the deviation of the best-line fit and account not for systematic errors, see the Supporting Information for further details.

[27] All computations were done with Gaussian 03, Revision B.03, M. J. Frisch, G. W. Trucks, H. B. Schlegel, G. E. Scuseria, M. A. Robb, J. R. Cheeseman, J. A. Montgomery, Jr., T. Vreven, K. N. Kudin, J. C. Burant, J. M. Millam, S. S. Iyengar, J. Tomasi, V. Barone, B.

Mennucci, M. Cossi, G. Scalmani, N. Rega, G. A. Petersson, H. Nakatsuji, M. Hada, M. Ehara, K. Toyota, R. Fukuda, J. Hasegawa, M. Ishida, T. Nakajima, Y. Honda, O. Kitao, H. Nakai, M. Klene, X. Li, J. E. Knox, H. P. Hratchian, J. B. Cross, V. Bakken, C. Adamo, J. Jaramillo, R. Gomperts, R. E. Stratmann, O. Yazyev, A. J. Austin, R. Cammi, C. Pomelli, J. W. Ochterski, P. Y. Ayala, K. Morokuma, G. A. Voth, P. Salvador, J. J. Dannenberg, V. G. Zakrzewski, S. Dapprich, A. D. Daniels, M. C. Strain, O. Farkas, D. K. Malick, A. D. Rabuck, K. Raghavachari, J. B. Foresman, J. V. Ortiz, Q. Cui, A. G. Baboul, S. Clifford, J. Cioslowski, B. B. Stefanov, G. Liu, A. Liashenko, P. Piskorz, I. Komaromi, R. L. Martin, D. J. Fox, T. Keith, M. A. Al-Laham, C. Y. Peng, A. Nanayakkara, M. Challacombe, P. M. W. Gill, B. Johnson, W. Chen, M. W. Wong, C. Gonzalez, J. A. Pople, Gaussian, Inc., Wallingford CT, **2003**.

[28] a) A. D. Becke, *Phys. Rev. A* **1988**, *38*, 3098; b) C. Lee, W. Yang, R. G. Parr, *Phys. Rev. B* **1988**, *37*, 785; c) A. D. Becke, *J. Chem. Phys.* **1993**, *98*, 5648; d) B. G. Johnson, P. M. W. Gill, J. A. Pople, *J. Chem. Phys.* **1993**, *98*, 5612.

[29] a) M. Head-Gordon, J. A. Pople, M. J. Frisch, *Chem. Phys. Lett.* **1988**, *153*, 503; b) M. J. Frisch, M. Head-Gordon, J. A. Pople, *Chem. Phys. Lett.* **1990**, *166*, 275; c) M. J. Frisch, M. Head-Gordon, J. A. Pople, *Chem. Phys. Lett.* **1990**, *166*, 281.

[30] M. Head-Gordon, T. Head-Gordon, *Chem. Phys. Lett.* **1994**, *220*, 122.

[31] a) J. Cizek, *Adv. Chem. Phys.* **1969**, *14*, 35; b) G. D. Purvis, R. J. Bartlett, *J. Chem. Phys.* **1982**, *76*, 1910; c) G. E. Scuseria, C. L. Janssen, H. F. Schaefer III, *J. Chem. Phys.* **1988**, *89*, 7382; d) G. E. Scuseria, H. F. Schaefer III, *J. Chem. Phys.* **1989**, *90*, 3700.

[32] a) D. E. Woon, T. H. Dunning, Jr., *J. Chem. Phys.* **1993**, *98*, 1358; b) R. A. Kendall, T. H. Dunning, Jr., R. J. Harrison, *J. Chem. Phys.* **1992**, *96*, 6796; c) T. H. Dunning, Jr., *J. Chem. Phys.* **1989**, *90*, 1007.

[33] Calculated from single point calculations at the B3LYP/6-311G-(2d,p) or MP2/6-311G(2d,p) level using the two optimized structures obtained at with the different methods.

[34] A summary of the results of computations using several correlation methods and density functionals along with different basis sets for a model cation is given in the Supporting Information.

[35] a) C. S. Griffith, G. A. Koutsantonis, B. W. Skelton, A. H. White, *J. Chem. Soc. Chem. Commun.* **2002**, 2174; b) U. Rosenthal, *Angew. Chem.* **2003**, *115*, 1832; *Angew. Chem. Int. Ed.* **2003**, *42*, 1794.

[36] The dynamic in protonated acetylene **3** is usually described as a degenerate rotation of the protons around the dicarbyne unit. The opposite point of view, to characterize the fluxional behavior as the rotational motion of the dicarbyne within the triangle of the fixed protons, is, however, valid as well.

Received: March 26, 2009